DETAILED CALIBRATION OF EDDY VISCOSITY TURBULENCE MODELS FOR INCIPIENT CAVITATING FLOW PREDICTIONS IN ASYMMETRICAL NOZZLE OF INJECTORS/ATOMIZERS

Miguel G. Coussirat[a], Flavio H. Moll[a], Alfred Fontanals[b]

[a]*Grupo UTN LAMA- Universidad Tecnológica Nacional - Facultad Regional Mendoza, Argentina, miguel.coussirat@frm.utn.edu.ar, http://www.frm.utn.edu.ar*
[b]*Departamento de Mecánica de Fluidos, Escola Enginyeria Barcelona Est, EEBE. Universitat Politècnica de Catalunya, Spain, alfred.fontanals@upc.edu, https://eebe.upc.edu/es*

Keywords: Cavitation; Injectors; Atomizers; Turbulence; Eddy Viscosity Models; Validation/Calibration.

Abstract: Cavitation in pressure injectors/atomizers strongly affects the liquid/spray jet behavior at its outlet. The type of atomization induced by cavitation allows developing more efficient devices if this cavitation state is controlled. Cavitating flow is related to turbulent and multiphase flows with mass transfer between the liquid and its gaseous phase. It is affected by several factors such as local pressure, local state of the turbulence, non-condensable dissolved gas concentration, nozzle geometry and others. Due to the high speed flow and small spatial and time scales involved, the study of cavitating flows by physical experiments is very expensive. On the other hand, several codes for numerical modeling of cavitating flows have been developed, but turbulent multiphase flow modeling is still a big challenge. Previous works showed that it is possible to capture several of the incipient cavitating flow characteristics performing a careful calibration of the Eddy Viscosity Models in nozzles with symmetrical inlet geometry and with round or square outlet sections. This work extends the study to nozzles with asymmetrical inlet geometry and square outlet section. It was demonstrated in previous works that a careful calibration task should be necessary, because there is a close relation between the cavitation inception/developing condition and the turbulence level in the flow leading to a 'non-standard turbulence state'. The spatial distribution and the slow decay of the turbulence level produced by cavitation could be related to some preferred turbulence scales in the process, so cavitating flows should not be modeled as typical turbulence. It is showed that based on the special characteristics of the incipient/slightly developed cavitating flows, a suitable calibration of the turbulence models allows obtaining improved results. These results become competitive when they are compared against ones computed by Large Eddy Simulations which need a lot of computational resources and an appropriate initial solution for running. It was also demonstrated that suppressing by calibration the level of the eddy viscosity in certain zones the vapor fraction predicted rises, provoking the incipient cavitation state in the flow. The obtained conclusions could be useful to improve injectors design using numerical modeling, because the detection of the incipient cavitation flow condition, useful to improve the atomization, could be captured accurately.

1. INTRODUCTION

The occurrence of cavitation inside a nozzle of a fuel injector for Diesel engines is directly connected with the local pressure drop. Understanding the cavitating flow phenomenon in a nozzle of a fuel injector has major importance, since it plays a significant role in the fuel spray atomization, which strongly affects Diesel engines performance and emissions. Cavitation is a complex phenomenon that appears in liquid flows when the hydrodynamic pressure, p_c in some place falls down reaching the vapor pressure of the liquid, p_v. This low pressure level provokes that the initial liquid flow becomes a two-phase flow, i.e., liquid-bubbles of vapor. The initiation of cavitation by liquid vaporization may require the existence of stresses lower than vapor pressure due to the surface stress tension in the bubble. However, the presence of undissolved gas particles, boundary layers, and turbulence will modify and often mask a departure of this critical pressure p_c from p_v. A complete set of details related with the cavitation phenomenology and bibliography related to this subject can be found in Coussirat et al., 2016-2018.

Computational Fluid Dynamics (CFD) codes based on a certain kind of 'multi-phase flow modeling' technique, involving both mass transfer and turbulence submodels have been specifically adapted/developed for studying cavitating flows. For turbulence modeling Reynolds Averaged Simulations plus Eddy Viscosity (or Reynolds Stress) Models, i.e., RAS+EVM(RSM) formulations for the mixture (liquid+vapor) have also been developed in the last two decades, being now a common option for CFD works. For cavitating flow the Transport Equation-Based modeling (TEM) is used, coupled with the aforementioned RAS+EVM(RSM) formulations. TEM consists in solving a transport equation for either mass and volume fraction, with appropriate source terms for regulate the transfer between phases. These models combination is frequently so-called RAS turbulent multiphase flow modeling (RAS/EVM-TMF/TEM), and several EVM and.formulations are currently available, see full details and references in Coussirat et al., 2016-2018.

This work is related to CFD modeling of cavitating flows in confined geometries, more specifically, dealing with high-pressure Diesel injectors with an asymmetrical nozzle inlet configuration and square sections at the outlet, see Fig.1. The main subject here is to gain a deeper insight in the behavior and performance of RAS/EVM-TMF models developed for general usage, when they are applied to design devices where cavitating flows appear. Previous works showed that a EVMs calibration is a necessary task and it must rely on a physical basis, Coussirat et al., 2016-2018. To discuss with more details the physical basis of the turbulence and cavitation interaction some of the experiments used in the quoted works were revisited. Both the mean velocity field and its fluctuations from Sou et al., 2014, Biçer et al., 2014 and Biçer 2015 experiments were used for the calibration tasks.

1.1 Phenomenology of cavitating flow in an asymmetrical nozzle

Several classical databases related to symmetrical inlet nozzles with different outlet sections exist, and a broad discussion and references related to the phenomenology of the cavitating flow in these nozzles can be seen in Coussirat et al., 2016-2018. More recently, information related to asymmetrical inlet nozzles are also available, e.g., Sou et al., 2007-2014, Biçer et al., 2014 and Biçer 2015. In these databases, detailed measurements of the velocity and turbulence, very useful for CFD codes calibration, were carried out. The experimental setup consisted in using a plunger pump to discharge filtered tap water at an ambient temperature of 19C into ambient air through a rectangular nozzle, Fig.1. The width (w_{out}), length and thickness of the nozzle were 1.98, 8 and 1.98 mm, respectively. The width of the upstream region (inlet) is four times as wide as the nozzle width. The liquid flow rate was measured using a flow-meter inserted in the hydraulic circuit. Upstream of the nozzle the static pressure was measured, but the exact position of this pressure (gauge) probe was not clearly defined in the experiments.

The mean stream-wise velocity, c_m and its RMS fluctuation c'_{RMS}, (both in the y direction) were measured using an Laser Doppler Velocimeter (LDV) system at three positions (y_1=-1.5, y_2=-3.0, y_3=-6.0mm, respectively) in the middle plane in depth of the nozzle channel, marked in the side view on the Fig.1. The uncertainty reported in the measurements was of ~1% for the LDV and of ~3.7% for the flow rate. Unfortunately, both the vapor fraction level into de cavity and local pressure measurements were not measured.
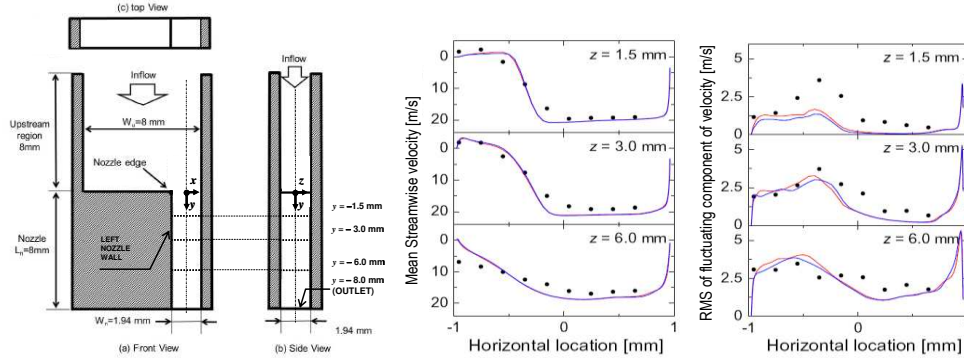

Fig.1. Geometry, boundary conditions, experimental and CFD mean c_m and RMS fluctuating c'_{RMS} velocity profiles, Reynolds number, Re=27,700, see Fig.2. **Nomenclature**: •, Experiments (LDV); CFD Smagorinsky (Red) and Vreman (Blue) LES SGS models respectively, Sou et al., 2007-2014 and Biçer 2015.

For no cavitation and incipient cavitation conditions, still images of cavitation and a liquid jet were taken by using a digital camera (Nikon, D70, 3008/2000 pixels) and a flash lamp (Nissin Electronic, MS-1000 and LH-15M, duration = 4μs). For full developed cavitation conditions, their evolution were captured using a high speed camera (Redlake, Motion Pro HS-1, frame rate = 20,000fps, exposure time = 50μs) and a reflector lamp (Panasonic, PRF-500), see details in Sou et al., 2007-2014 and Biçer 2015. The flow separation occurs only at the sharp-edged inlet of the nozzle (the step) and the incipient cavitation condition appears only along the left nozzle wall in zones nearer the step, Fig.2.
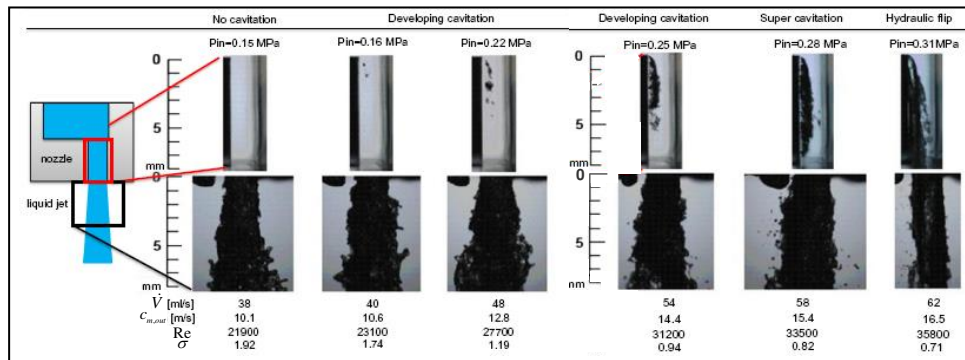

Fig.2. Cavitating flow patterns (Sou et al., 2014 and Biçer 2015). **Nomenclature**: σ, Re, Cavitation and Reynolds numbers, Eq.1; p_{in}, inlet pressure; p_{out}, outlet pressure (=1.0e+5Pa); p_v, vapor pressure (=2,300Pa); ρ, liquid density (=998kg/m^3); $c_{m,out}$, outlet mean velocity; w_{out}, nozzle width; ν, liquid viscosity (=1.35e-6m^2/s).

Different cavitation conditions were generated changing the flow rate. The outlet pressure p_{out} remains constant and equal to atmospheric pressure, because the nozzle outlet is a free jet (subsonic flow and negligible surface stresses). In this way, the states from no cavitation till hydraulic flip (flipping flow) were reproduced. All of them can be classified by the Reynolds and the Cavitation numbers computed from Eq.1, highlighting here that Re and σ numbers are not closely related, Sou et al., 2008, being both necessary for this flow classification. In the Fig.2 caption, both the flow structure and the notation/meaning of the variables from the

Eq.1 are clearly explained. When the σ value is decreased (i.e., the flow rate is increased), see Fig.2, a huge number of bubble nuclei starts to grow and vortices fly off from the detachment point in the low pressure zones within the recirculation region. The vortices are accompanied by clouds of bubbles that collapse during the shedding when downstream the pressure rises again.

$$\text{Re} = c_{m,out}w_{out}/\nu \ ; \qquad \sigma = (p_{out} - p_v)/(0.5\rho c_{m,out}^2) \tag{1}$$

It can also be observed that this transition has a quite unsteady behavior, probably due to the short length of the nozzle, being this fact an added difficulty for the CFD modeling.

In previous works dealing with cavitating flows, Coussirat et al., 2016-2018 showed that it is possible to capture several of the incipient cavitating flow characteristics, by means of a careful calibration of the EVMs in nozzles with round and square outlet section and with symmetrical inlet geometry. It was demonstrated that a special calibration task is necessary, due to the close relation between the cavitation inception/developing condition and the turbulence level in the flow. The spatial distribution and the decay rate of the turbulence level produced by cavitation could be related to some preferred turbulence scales in the process, leading to a 'non-standard turbulence state'. So cavitating flows should not be modeled as typical turbulence, Coussirat et al., 2016a, Coussirat 2016b. Commonly, uncalibrated EVMs overpredict the μ_t level that leads to lower values for the dynamic pressure yielding a higher absolute pressure value and less cavitation. This μ_t overestimation affects directly the cavitation region due to the high stresses computed, limiting both cavitation and velocity distribution in recirculation zones, Shi et al., 2010, Biçer et al., 2014, Coussirat 2016a. It was also demonstrated by Coussirat et al., 2016-2018 that in general there is a higher dependence on the obtained results for the incipient cavitation state, associated with the EVM used for turbulence modeling than on the cavitation models. The cavitation models used have shown slight differences in the cavity shape and vapor fractions levels predicted.

Because real injectors have not symmetry at their inlets in several cases, this work extends the study to asymmetrical inlet geometries, Fig.1. Under this situation the flow inside the nozzle has a different pattern than in a symmetrical nozzle. Other goal of this work is to compare LES results against ones obtained by EVMs. It is known that LES modeling allows obtaining a more detailed cavity shape in cases of slightly developed cavitation, but it requires more computational (CPU) resources. The question here is: 'is it possible to obtain a sufficient resolution in the cavity shape at an incipient cavitation state by using EVMs?' The main goal of this work is to give an answer to this question, and the work started with a bibliographic survey to obtain more recent experimental databases and CFD results.

Sou et al., 2014 and Biçer 2015 presented experimental and CFD results (EVMs and LES simulations) in an asymmetrical nozzle configuration, Fig.1, using the combination of Lagrangian Bubble Tracking Method (BTM), a Modified Rayleigh Plesset equation (MR) and LES. Two kind of LES Sub Grid Scale (SGS) models (i.e., Smagorinsky and Vreman) were used. This combination was applied only to incipient cavitation conditions, giving a good prediction for the cavitation length, thickness and for the cavitation cloud shedding. However, it required a very fine grid and a lot of computational time.

To simulate the turbulent flow under unsteady conditions by using RAS/EVM option also, three EVM turbulence models, (the Standard k-ε, the SST k-ω and RNG k-ε) were investigated by these authors. It is highlighted that Biçer 2015 uses the Standard Wall functions for the EVMs selected and the Van Driest damping for the LES modeling, like as Sou et al., 2014. They concluded that RNG k-ε model with MR equation gave a good prediction for the cavitation length and thickness using a locally refined grid with a minimum length cell of $h\sim50\mu m=0.05mm$ (compare against the cell size of meshes from Table.1). The

cavitation cloud shedding was well reproduced by the MR/RNG k-ε (or the SST k-ω) models using the mesh with h<50μm and time steps of $O(10^{-8}$s). In cases of developed cavitation the cloud shedding was well simulated too. Both the recirculation flow and the vortex shedding accompanied by a cavitation cloud until the nozzle exit were well captured with the combination of the MR/LES models using a fine grid with a minimum mesh cell size of h~4.4μm compared to the EVMs. The study concluded that the MR equation combined with an appropriate turbulence model (EVM or LES) and using a very fine mesh can simulate the complex cavitating recirculation flow, the cloud cavitation shedding and the re-entrant jet flow. This combination can simulate cavitation thickness, the cavity length, the mean and the fluctuating turbulence velocities quantitatively too. Afterwards, this combination could be used to explore cavitation phenomena inside fuel injector nozzles. The main problem remains in the high CPU requirements for these unsteady simulations.

2. METHODOLOGY DEVELOPED FOR STUDYING CAVITATING FLOWS

In this work, the main goal is to check the possibility of detecting incipient cavitation obtaining some information related to the cavity shape by means of a steady simulation using EVMs. Then, to compare against the aforementioned experimental/CFD results to the ones that will be obtained here by calibrated EVMs, the following methodology was defined, namely: 1)To perform a detailed study of grid independence of the results obtained using the Grid Convergence Index (GCI) combined with the Richardson extrapolation techniques for a no cavitation state, i.e., σ=1.91, see details in Ali et al., 2008, Celik et al., 2008, Xing et al., 2010 and Roache 2011. 2)To perform a detailed EVMs calibration using the previous results obtained in Coussirat et al., 2016-2018 for a developing (incipient) cavitating flow (σ=1.19).
The possibility of steady flow CFD simulations was checked by means of computing the Strouhal number, Sr=$L_\sigma(c_\sigma t)^{-1}$ being L_σ, t and c_σ the characteristic length, time and velocity scales of the unsteadiness respectively. A broad discussion to define suitable values for these scales was presented in Dular et al., 2009 and Coussirat et al., 2017. This leads to take the following values for σ=1.19: L_σ ~$O(w)$=1.98mm; t=0.01s and $c_\sigma = c_{m,out}\sqrt{1+\sigma} = 18.9 m/s$, leading to compute a Sr =0.01. Then, the selected cases could look like as a steady phenomenon correlated to low shedding frequencies under an incipient cavitation state.

2.1 Turbulence and cavitation models selected

Four EVM turbulence models were used, i.e., the Spalart Allmaras (SA), the Standard k-ε (Ske), the SST k-ω (SST) and the RNG k-ε (RNG). Full details and references for all these models can be seen in Versteeg et al., 2007 and Ansys, 2008. Here, the flow is an undeveloped flow, therefore a previous estimation of cell size needed, based in a value of y+ =15 was made to avoid the use of wall functions in the selected EVMs that require this strategy. For the cavitation modeling the TEM model from Shingal et al., 2002 was selected, because in previous works this model shows a good performance, see details in Coussirat et al., 2016-2018.

2.2 Geometry, Boundary Conditions and Discretizations schemes defined

On the selected geometry, Fig.1, five homogeneous successively refined grids with a cell area of $h \times h$, were built, see Table.1. The inlet boundary condition was defined as a mean value for the inlet velocity. This value was computed from the mass conservation principle, because the outlet velocity for each case and both the inlet and outlet sections are known in advance. The turbulence boundary conditions were computed from standard formulations for each EVM, see details in Versteeg et al., 2007. At the outlet a defined pressure value was imposed

(=1.0e+5 Pa) and a no-slip condition was defined at the walls. The selected discretisation schemes were: QUICK for the density, the vapor fraction, momentum equations and turbulent quantities, PRESTO! for the pressure and SIMPLEC for the pressure-velocity coupling, see details in Versteeg et al., 2007 and Ansys, 2008. After the CFD modeling, the predicted inlet pressure and de corresponding σ value were verified for each case, see Fig.2.

	M05	M04	M04(3D)	M03	M02	M01
h [mm]	0.16	0.08	0.08	0.04	0.02	0.01
Cells [Adim]	3,600	12,300	326,400	50,000	198,800	795,200
$y^{+}{}_{m}$ [Adim]	13.27	12.40	11.63	5.91	3.02	1.53

Table.1. Meshes defined. **Nomenclature**: h, cells side; $y^{+}{}_{m}$, averaged local Re along the left nozzle wall, Eq.2.

2.3 Grid sensitivity study performed

It is very important in a CFD study to know what kind of information is needed, because different parameters will converge differently. When a higher order parameter is being computed/predicted, such as the local wall friction, the grid requirements might be stricter than the ones required for an integral quantity (i.e., lower order parameters) such as the mean pressure, the mean velocity or the drag coefficient. If it is necessary to analyze both high and low order properties in a simulation, then a very rigorous grid convergence study of primitive, integrated and derived variables is mandatory (Ali et al., 2008, Celik et al., 2008, Xing et al., 2010, Roache 2011).

Taking into account the advices from Roache 1997 concerning the turbulent flow modeling in confined flows, a grid convergence study was performed for the SA, the Ske and the SST EVMs to have some guaranty of grid independence in the computed results by these models. Initial simulations for no cavitating flow state (σ =1.91, see Fig.1) were carried out for each of the selected EVMs. The GCI method combined with the Richardson extrapolation was applied to check the uncertainty in the selected variables. The aforementioned five successively refined grids were used, by taking three sets, each of them with three consecutively refined grids (i.e., sets M05-03, M04-02, M03-01, see Table.1). Also, to verify both the local and the mean $y+$ values along the nozzle wall, previously computed by hand, a preliminary CFD computation were performed using the SA model. Global mass conservation was checked in all the simulated cases by computing the relative difference between the inlet/outlet mass flows too. The values computed for the GCI study were for the: ϕ_1, ϕ_2 (=c_m), mean pressure and mean velocity respectively (both at position y_3); ϕ_3 (=$c_{m,out}$) outlet mean velocity (related to the outlet flow rate) and ϕ_4 (=$y^{+}{}_{m}$) an ad-hoc defined parameter, Eq.2 (an "averaged" Re along the left nozzle wall, Fig.1).

$$y_m^{+} = \phi_4 = \frac{1}{N_h} \sum_{i=1}^{N_h} \left[x_i \sqrt{\tau_{w,i} / \rho} / \nu \right] . \tag{2}$$

Being: ρ, ν, density and viscosity of the liquid phase respectively; N_h, the cells along of the left nozzle wall; x_i, the distance from this wall to each cell centre and $\tau_{w,i}$, the local wall stress at each cell. The GCI results obtained for ϕ_3 can be seen in Fig.3, where the h values in this figure can be associated to the corresponding cell size in each grid showed in Table.1.

For all the EVMs used, the asymptotic range was reached for the ϕ_1, ϕ_2, and ϕ_3 in the sets M05-03 and M04-02. Instead, ϕ_1 reaches the asymptotic range only in some cases in the set M03-01. On the other hand, the variable ϕ_4 never reaches a clear asymptotic range, being this behavior expected, because this variable is closely related to the grid size. The variables ϕ_2, ϕ_3 and ϕ_4 showed a monotonic convergence, but the variable ϕ_1 showed an oscillatory

convergence in some cases. It is remarked that asymptotic values computed by the Richardson's extrapolation (i.e., for *h*=0) show some variations, depending on the grid set used (i.e., M05-03, M04-02, M03-01), see Fig.3. The behavior of ϕ_l could be correlated with the $O(10^{-6})$ obtained difference between the inlet and the outlet flow rate, when the M05-M02 meshes were used. Instead, for the grid M01 the flow rate difference only reached an $O(10^{-4})$ and the computed pressure field showed some instability too. The predicted level of the pressure oscillations were of an $O(10^{-2})$, i.e., an $O(10^{+3})$ around the mean value of the pressure, i.e., ~9.5e+5 ± 5.0e+3Pa, at position y_3, a phenomenon not observed in the other grids. The observed pressure unsteadiness provokes an artificial shedding that affects the order of convergence in the mass flow and could be related to the Near-Wall Modeling (NWM) involved in all the EVMs used. It is highlighted that this unsteadiness was not observed when the M05-M02 grids were used for computations.
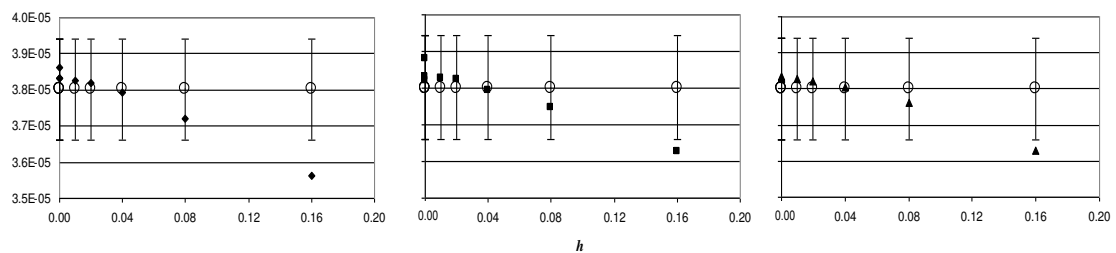

Fig.3. GCI study: flow rate [m³/s] computed vs cell size *h* [mm], experiments from Sou et al., 2014 and Biçer 2015. **Nomenclature**: ○, Exp. (vertical bars point out the experimental uncertainty);▲,SA; ♦, Ske; ■, SST.

A possible explanation for this behavior could be that the incipient cavitation starts for this σ value, being the grid M01 more sensitive to this phenomenon, despite the experiments do not show any clear cavitating flow pattern. Notice that the changes observed in the velocity were only of an $O(10^{-2})$ for an $O(10^{1})$ mean velocity. Then, these levels of variations in the predicted pressure ϕ_l could be responsible for the predicted cavitation onset (or not), being the pressure a variable more sensitive than the velocity to the NWM strategy selected and correlated to some kind of grid dependence (Roache 1997, Coussirat 2016a). Therefore, the correlation between pressure fluctuations and turbulence could play a role of paramount importance here. More detailed investigations will be necessary to solve this uncertainty. A future work could explain why the results obtained do not reach the asymptotic range for ϕ_l when the M03 grid is used in set M03-01. Unfortunately, there are not experimental ϕ_l values for comparison, being this fact an added difficulty for performing the involved EVMs calibration tasks of this future work.

Despite the difficulties aforementioned, this GCI check allows saying with some confidence that the grid M03 has sufficient resolution for the subsequent incipient cavitation state modeling task. Here, the RNG turbulence model was added to study its performance under this cavitation condition, comparing its results against ones from Biçer 2015.

Likewise, to check the quality of the solution Two- and Three dimensional cases were also computed using the 2D M04 grid and then, extending this grid to a 3D case. Simulations for these grids, using the SA model does not show strong differences when the results are compared at the 3D mid plane and the 2D cases. The 3D solution showed a mass conservation of only an $O(10^{-4})$ against the $O(10^{-6})$ observed in the 2D case. In the 3D case, a clear symmetry in the central plane for both the velocity and pressure fields was also observed (not shown here). Some 3D effects were observed only confined at the corner between the top/bottom walls and the step and they do not affect the general flow pattern. The comparison carried out allows saying that there is not a strong difference between the 2D and 3D results obtained. A similar behavior for the 3D M03 grid should be expected. Therefore, 2D

simulations will be performed for EVMs checking/calibration for the developing (incipient) cavitation state (i.e., σ =1.19).

3. STUDY OF THE INCIPIENT CAVITATION STATE IN THE NOZZLE

For the grid M03 an incipient cavitation state (σ =1.19, see Fig.1) was firstly modeled using the default values for all the calibration parameters of the selected EVMs and secondly, modeled by the calibrated SST model. After that, comparisons between experiments and CFD simulations were performed for: 1)the averaged c_m at the outlet i.e., $c_{m,out}$, Table.2; 2)c_m and c'_{RMS} profiles at positions y_1, y_2, y_3, see Fig.4; 3)the cavity shape (vapor fraction), see Fig.5.

Table.2 shows that all the used EVMs underpredict the $c_{m,\,out}$ when the default calibration values were used. The SA model gave the best result and conversely, the worse prediction was given by the SST model. Then, the SST model was calibrated by changing the parameter β^*_∞, being this parameter responsible for the computed level of the production and the dissipation of the kinetic energy k, see full details in Coussirat et al., 2017. Under this fine tuning of β^*_∞, it was observed that the $c_{m,\,out}$ predictions are better, but for β^*_∞ >0.12 some oscillations in the computed $c_{m,out}$ appear, despite the improvement obtained.

Exp.	SA	Ske	RNG	SST (β^*_∞=0.09, default)	SST (β^*_∞=0.11)	SST (β^*_∞=0.18)
12.800	12.754	12.727	12.745	12.724	12.734	12.790
Error (%)	0.36	0.57	0.43	0.59	0.51	0.08

Table.2. CFD results (M03, σ =1.19): Mean velocity (c_m) averaged at the outlet, $c_{m,out}$, [m/s].
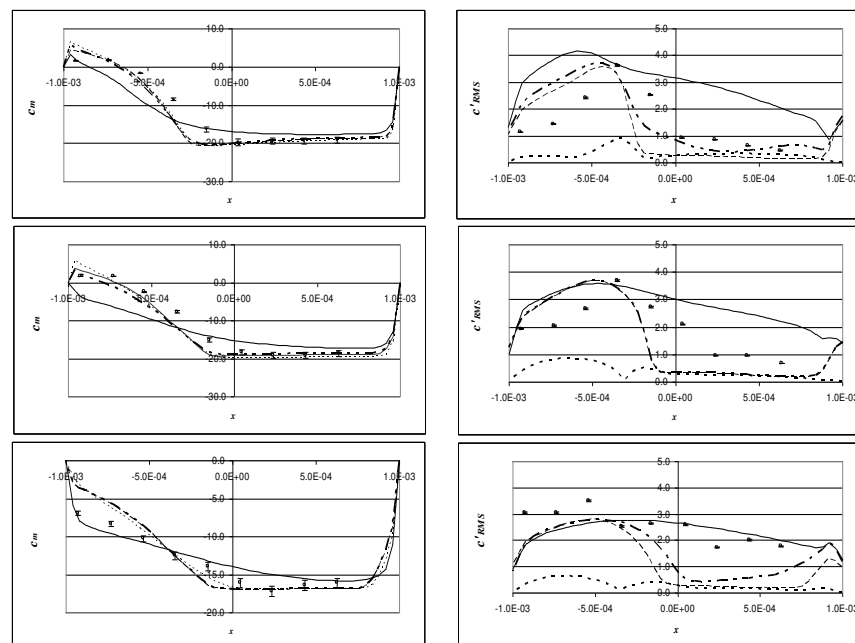

Fig.4. CFD results (M03, σ =1.19): Velocity profiles: c_m (left) and c'_{RMS} (right). **Top**: y_1, **Middle**: y_2, **Bottom**: y_3. **Nomenclature**: x [mm], horizontal coordinate (nozzle);·, Exp. (Sou et al., 2014 and Biçer 2015, vertical bars point out uncertainty); -----,SA; ——, Ske; – – –, SST; –··–RNG.

Fig.4 shows that the models SA, SST and RNG give similar quite good predictions for the c_m profiles at these positions. At y_1 and y_2 the Ske model overpredicts the c_m profile in zones nearer the left wall of the nozzle (x<0) and the profiles are smoother than the ones predicted by the other EVMs. Comparison against LES results from Fig.1 shows a similar quality for the c_m adjustments. On the other hand, the c'_{RMS} profiles were strongly underpredicted by the SA

model at all the positions. At y_1 and y_2 the SST model gives the best fitting for the c'_{RMS} profiles. The Ske model overpredicts the c'_{RMS} profile when $x>0$. At y_3 the c'_{RMS} predictions are improved by the Ske model, but conversely the results from the models SST and RNG become worse here.

In order to check if calibration allows saving CPU resources, comparisons were carried out against: 1)the Biçer 2015 results computed in selectively refined grids (73,200-621,020 cells) using EVMs, 2)the Sou et al., 2014 and Biçer 2015 results computed by using the LES Smagorinsky and Vreman's SGS models, see Fig.1. These LES results needed time steps of $O(10^{-8})$, about 700,000 cells for a precursor simulation (to obtain an inlet boundary condition) and 2,800,000 cells in the nozzle simulations involving high CPU requirements.

The comparison (not shown here) between results from the models RNG and SST (uncalibrated) obtained here and the ones from Biçer 2015 have the same quality. The calibrated SST model improves these results, despite the coarser grid used. The comparison between Fig.1 and Fig.4 shows both a similar quality for the predicted c_m profiles and a clear improvement of the c'_{RMS} profiles predicted concluding that it is possible to obtain RAS/EVMs results of similar quality as the LES simulations, but saving a lot of CPU resources by means of GCI study+EVM calibration. Fig.5 shows the general shape of the cavity predicted by the SST model when the calibration parameter β^*_∞ is changed. The red frame remarks the measurement zone/computational domain, because in the experiments the acrylic front wall introduces some distortions in the nozzle image. It was demonstrated that an improvement in the computed results was obtained by means of a GCI study joined to a careful calibration for the SST model.
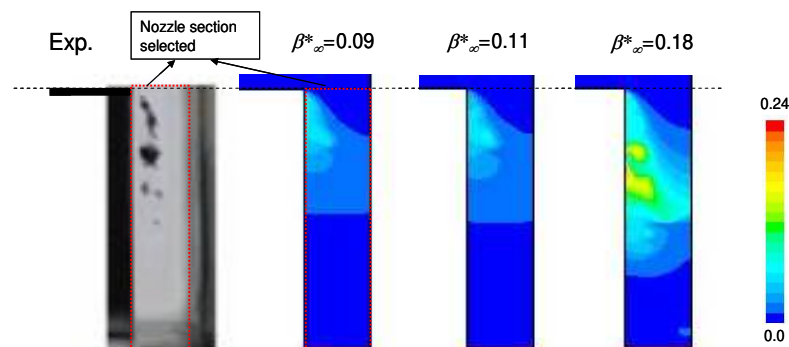

Fig.5: CFD results (M03, σ=1.19): Cavity shape (vapour fraction). **Nomenclature**: Exp., Experiments Sou et al., 2014; Red frame, measurement/CFD domain; β^*_∞, calibration parameter, SST model.

It is shown that depending on the selected value for β^*_∞, the μ_t is suppressed at y_1 leading to a rising in the vapor fraction. Therefore, the unsteady nature of cavitation in this geometry is captured despite the steady simulation performed, because: 1)the 'incipient shedding' is better observed; 2)the $c_{m,out}$ prediction becomes better, see Table 2; 3)fluctuating velocity field, c'_{RMS}, at the nozzle inlet is slightly better adjusted when $\beta^*_\infty>0.09$ (not shown here). Unfortunately, in the experiments the vapor fraction level was not measured and only its shape could be compared against CFD results.

4. CONCLUSIONS

A set of four EVMs were used for modeling a developing (incipient) cavitation state, σ=1.19 in an asymmetrical inlet/square outlet section nozzle configuration after a careful GCI study+EMVs calibration. Quite good prediction of c_m and c'_{RMS} were obtained demonstrating that it is possible to obtain similar results as LES modeling saving a lot of CPU resources.

A detailed calibration of the SST model allows improving both the fitting of the fluctuating velocity field c'_{RMS}, in zones nearer the step (i.e., nozzle inlet) and the cavity shape. A good

fitting of this field is necessary for a more accurate cavity shape prediction, because the mean velocity field c_m does not suffer strong variations when the calibration is performed, but the c'_{RMS} field predicted is strongly affected by calibration. This fact remarks the close relation between the turbulence level and the cavitation inception phenomenon, because it was demonstrated that suppressing by calibration the μ_t level the vapor fraction predicted rises.

A more detailed investigation will be necessary to explain why the results obtained do not reach the asymptotic range for ϕ_I when the grid M01 is used. The NWM could be responsible of this deficiency, because the computed pressure fluctuations which are correlated to the μ_t level predicted in zones nearer the nozzle inlet could play a role of paramount importance in the cavity development, being necessary a more accurate turbulence modeling here.

5. AKNOWLDEDGEMENTS

REFERENCES

Ali M., Doolan C., Wheatley V., Convergence Study for a Two-Dimensional Simulation of Flow Around a Square Cylinder at a Low Reynolds Number, *Seventh International Conference on CFD in the Minerals and Process Industries CSIRO*, Australia, 2009.

Ansys/Fluent Software, 2018, http://www.ansys.com/Industries/Academic/Tools/

Biçer B., Numerical Simulation of Cavitation Phenomena inside Fuel Injector Nozzles, *PhD Thesis*, *Kobe University*, Japan, 2015.

Biçer B., Sou A., Numerical Simulation of Turbulent Cavitating Flow in Diesel Fuel Injector, *Proceedings of the 3rd Intern. Symp. of Maritime Scie.*, *Nov.10-14*, Kobe, Japan, 2014.

Celik I., Ghia U., Roache P., Freitas C., Coleman H., Raad P., Procedure for Estimation and Reporting of Uncertainty Due to Discretization in CFD Applic., *J. Fluids Eng.*, 130(7), 2008.

Coussirat, M., Moll, F., Cappa, F., and Fontanals A., Study of Available Turbulence and Cavitation Models to Reproduce Flow Patterns in Confined Flows,", *J. Fluids Eng.*, 138(9), 2016,.

Coussirat M., Moll F. and Fontanals A., Capability of The Present Cavitating and Turbulence Models For Confined Flow Simulations, *Mec. Computac., Vol XXXIV*:1989–2007, 2016.

Coussirat M., Moll F. and Fontanals A., Reproduction of the cavitating flows patterns in several nozzles geometries using calibrated turbulence and cavitation models, *Mec. Computac., Vol XXXV*:819–841, 2017.

Coussirat M., Moll F. and Fontanals A., Cavitating flow pattern characterization in square section injectors by means of CFD, *Mec. Computac., Vol XXXVI*:1163–1172, 2018.

Dular, M., and Bachert, R., The Issue of Strouhal Number Definition in Cavitating Flow, *Journal of Mechanical Engineering* 55(11), 666-674, 2009.

Shi J. and Arafin M., CFD investigation of fuel property effect on cavitating flow in generic nozzle geometries, *ILASS–Europe2010, 23rd Ann. Conf. on Liquid Atomiz. and Spray Syst.*, Czech Republic, 2010.

Sou A., Biçer B., Tomiyama A., Numerical simulation of incipient cavitation flow in a nozzle of fuel injector, *Computers & Fluids* 103:42–48, 2014.

Sou A., Hosokawa S., Tomiyama A., Effects of cavitation in a nozzle on liquid jet atomization, *International Journal of Heat and Mass Transfer* 50: 3575–3582, 2007.

Sou, A., Maulana M., Isozaki K., Hosokawa, S. and Tomiyama, A., Effects of Nozzle Geometry on Cavitation in Nozzles of Pressure Atomizers, *J. Fluid Scie.Tech*. 3(5):622–632, 2008.

Singhal, A., Athavale, M., Li, H., and Jiang, Y., Mathematical Basis and Validation of Full Cavitation Model, *J. Fluids Eng.* 124(3):617–624, 2002.

Roache P., Quantification of Uncertainty in Computational Fluid Dynamics, *Annu. Rev. Fluid. Mech*. 29:123–160, 1997.

Roache P., Discussion: Factors of Safety for Richardson Extrapolation (Xing T., and Stern F.2010, ASME J. Fluids Eng.,132, pp.061403), *J. Fluids Eng.*, 133(11), 2011.

Xing T., Stern F., Factors of Safety for Richardson Extrapolation, *J. Fluids Eng.*, 132(6), 2010.

Versteeg H. and Malalasekera W. *An Introduction to Computational Fluid Dynamics: The Finite Volume Method.* 2nd Edition, Addison-Wesley, 2007.